Organic & Biomolecular Chemistry

PAPER

View Article Online
View Journal | View Issue

Cite this: *Org. Biomol. Chem.*, 2014, **12**, 5611

Hydroxyl radical induced oxidation of theophylline in water: a kinetic and mechanistic study†

M. M. Sunil Paul,[a] U. K. Aravind,[b] G. Pramod,[c] A. Saha[d] and C. T. Aravindakumar*[a,e]

Oxidative destruction and mineralization of emerging organic pollutants by hydroxyl radicals (•OH) is a well established area of research. The possibility of generating hazardous by-products in the case of •OH reaction demands extensive investigations on the degradation mechanism. A combination of pulse radiolysis and steady state photolysis (H_2O_2/UV photolysis) followed by high resolution mass spectrometric (HRMS) analysis have been employed to explicate the kinetic and mechanistic features of the destruction of theophylline, a model pharmaceutical compound and an identified pollutant, by •OH in the present study. The oxidative destruction of this molecule, for intermediate product studies, was initially achieved by H_2O_2/UV photolysis. The transient absorption spectrum corresponding to the reaction of •OH with theophylline at pH 6, primarily caused by the generation of (T8-OH)•, was characterised by an absorption band at 330 nm (k_2 = (8.22 ± 0.03) × 10^9 dm^3 mol^{-1} s^{-1}). A significantly different spectrum (λ_{max}: 340 nm) was observed at highly alkaline pH (10.2) due to the deprotonation of this radical (pK_a ~ 10.0). Specific one electron oxidants such as sulphate radical anions ($SO_4^{\bullet-}$) and azide radicals ($N_3^{\bullet}$) produce the deprotonated form (T(–H)•) of the radical cation ($T^{\bullet+}$) of theophylline (pK_a 3.1) with k_2 values of (7.51 ± 0.04) × 10^9 dm^3 mol^{-1} s^{-1} and (7.61 ± 0.02) × 10^9 dm^3 mol^{-1} s^{-1} respectively. Conversely, oxide radicals ($O^{\bullet-}$) react with theophylline *via* a hydrogen abstraction protocol with a rather slow k_2 value of (1.95 ± 0.02) × 10^9 dm^3 mol^{-1} s^{-1}. The transient spectral studies were complemented by the end product profile acquired by HRMS analysis. Various transformation products of theophylline induced by •OH were identified by this technique which include derivatives of uric acids (**i**, **iv** & **v**) and xanthines (**ii**, **iii** & **vi**). Further breakdown of the early formed product due to •OH attack leads to ring opened compounds (**ix–xiv**). The kinetic and mechanistic data furnished in the present study serve as a basic frame work for the construction of •OH induced water treatment systems as well as to understand the biological implications of compounds of this kind.

Received 14th January 2014,
Accepted 30th April 2014

DOI: 10.1039/c4ob00102h

www.rsc.org/obc

1. Introduction

Hydroxyl radicals (•OH) are the key species responsible for the oxidative destruction of environmental pollutants in many Advanced Oxidation Processes (AOPs) such as TiO_2 photocatalysis, H_2O_2/UV photolysis, sonolysis, γ-radiolysis *etc.*,[1–7] and many biological processes including DNA damage, mutation and ageing.[8–16] The •OH induced destruction of emerging organic pollutants has been widely experimented[1–4,7,17,18] since the presence of pharmaceutically active compounds in the aquatic environment became an emerging environmental issue.[19–22] Pulse radiolysis studies reveal that •OH reacts with a large number of organic molecules with a nearly diffusion controlled rate.[5,6,12,15,23,24] Furthermore, the ability to achieve complete mineralization[2,6] makes techniques of these kinds acceptable and environmentally friendly.

Conversely, recent studies using high resolution mass spectrometric (HRMS) techniques demonstrated that the formation of aromatic intermediates (that are likely toxic) as a

[a]*School of Environmental Sciences, Mahatma Gandhi University, Kottayam, India. E-mail: cta@mgu.ac.in*
[b]*Advanced Centre of Environmental Studies and Sustainable Development, Mahatma Gandhi University, Kottayam, India*
[c]*Department of Chemistry, N.S.S. Hindu College, Changanachery, India*
[d]*UGC-DAE Consortium for Scientific Research, Kolkata Centre, Kolkata, India*
[e]*Inter University Instrumentation Centre, Mahatma Gandhi University, Kottayam, India*

†Electronic supplementary information (ESI) available: The spectral and kinetic parameters of the reaction of •OH, $SO_4^{\bullet-}$, $N_3^{\bullet}$ and $O^{\bullet-}$ with theophylline (Table S1); MS and MS/MS spectra of selected transformation products (Fig. S1–S16); decay (320 nm, 350 nm) traces in the case of reaction of $O^{\bullet-}$ (Fig. S17); transient absorption spectrum of theophylline during its reaction with $SO_4^{\bullet-}$ and $N_3^{\bullet}$ at longer time scale (Fig. S18); UV-Vis spectrum of theophylline at pH 6.0 and 10.1 (Fig. S19); plot of absorbance of transient at 330 nm obtained by the reaction of theophylline with •OH against pH (Fig. S20); percentage degradation of theophylline in N_2 purged and aerated conditions as a function of time (Fig. S21). See DOI: 10.1039/c4ob00102h

result of $^{\bullet}OH$ attack is viable in the case of a number of organic compounds.[5,6,17,18] This could cause serious health problems on targeted organisms because of their potential biological activities. The kinetic and mechanistic investigation of the reaction mechanism, including the identification of the transient intermediate products as well as the stable transformation products, is thus very important in the case of any $^{\bullet}OH$ mediated destruction protocol prior to its implementation in a real system.

Theophylline (trade name: Deriphyllin), an extensively used drug for the therapy of different respiratory diseases such as chronic obstructive pulmonary disease (COPD), asthma *etc.*,[25–27] is used as a model compound for this study. It is naturally found in a variety of products such as cocoa beans (~3 mg g^{-1}), green tea (~0.5 g kg^{-1}), coffee, chocolate and cola beverages in variable amounts.[25–27] It is reported as a metabolite of caffeine[28] and a number of naturally occurring alkaloids.[29] It enhances the anti-inflammatory effect of steroids by increasing the histone deacetylase (HDAC) activity.[30] Theophylline is moderately toxic to mammals (LD_{50} > 200 mg kg^{-1}) such as mice, rabbits, rats *etc.*[31] and exhibits a negative (log *P* at pH 7 and 20 °C is −0.02) octane–water partition coefficient.[32] It is reported that higher doses of theophylline (>20 μg ml^{-1}) cause serious health problems (such as cardiac arrest, arrhythmias and hypotension) in humans.[25–27,33] A recent report by Antoniou and co-workers demonstrated that the toxicity of theophylline increases (around double) when it is administrated with Ciprofloxacin, a widely used fluoroquinolone antibiotic.[34] Furthermore, the presence of this compound in the aquatic environment has been recently reported.[21,22] Bioaccumulation and specific biological activities of pharmaceutically active compounds like theophylline makes them harmful to targeted organisms especially in the case of the aquatic environment.[21,22] Studies on the removal/degradation of this compound from aqueous medium is consequently a very relevant topic of investigation.

The destruction of this compound by one of the AOP techniques (photocatalysis) has been recently reported.[35] However, detailed information on the kinetic and mechanistic aspects of its reaction with $^{\bullet}OH$ is very limited.[36] An in-depth understanding of the kinetic and mechanistic aspects of the $^{\bullet}OH$ reaction of this compound is thus very necessary for the proper application of AOP techniques for the removal of this compound from water. A systematic investigation of the reaction of theophylline in aqueous medium using photolytically produced hydroxyl radicals (H_2O_2/UV) is carried out in the present study. The kinetics of this reaction and the formation of possible transient intermediate radicals have been probed using pulse radiolysis technique. In order to obtain more insight into the underlying reaction mechanism, the end products formed during the reaction were evaluated using a state-of-the-art mass spectrometric method. Additionally, a comparison of $^{\bullet}OH$ reaction of this compound, on the transient spectra and product profile, and with some other specific radicals ($SO_4^{\bullet-}$, $N_3^{\bullet}$ and $O^{\bullet-}$) was also carried out. An in-depth mechanistic understanding of the reaction of this compound with oxidizing radicals is very valuable in the case of Advanced Oxidation Technologies as well as in biological systems mainly due to the anti-oxidant properties of methylxanthines[28,36] and its structural similarities with purine bases.

2. Materials and methods

Theophylline (1,3-dimethyl-3,9-dihydro-1*H*-purine-2,6-dione, CAS no. 58-55-9) was purchased from Sigma Aldrich and was used as received. Potassium persulfate, 2-methyl-2-propanol, sodium azide and sodium hydroxide were obtained from Fischer Scientific. High purity N_2O and Ar gas was used for pulse radiolysis experiments. HPLC and LC-MS grade solvents were used for the HPLC and LC-Q-TOF-MS analysis respectively.

2.1. Steady state photolysis

Steady state photolysis experiments in the presence of hydrogen peroxide (H_2O_2/UV photolysis) were carried out on a photo reactor supplied by Scientific Aids & Instruments Corporation (SAIC, Chennai). The reactor utilizes a 125 W medium pressure deuterium lamp as the light source, which is kept in a quartz vessel. The lamp emits a continuous light spectrum between 185 nm to 400 nm region. All the experiments were carried out at near natural pH (~6) and room temperature.

2.2. HPLC analysis

The variation in the concentration of theophylline after H_2O_2/UV photolysis was monitored by using a Shimadzu LC-20AD Prominence Liquid Chromatography system coupled with a Diode Array Detector (at 270 nm). An isocratic elution of methanol and water (25 : 75) at a flow rate of 0.8 mL min^{-1} against an Enable C18G column (250 mm × 4.6 mm × 5 μm) was used as mobile phase.

2.3. LC-Q-TOF-MS analysis

The stable transformation products of theophylline formed during the reaction of $^{\bullet}OH$ were analyzed on a Waters Acquity H class UPLC system coupled with a Waters Xevo G2 Quadrapole-Time-of-Flight (Q-TOF) high resolution mass spectrometer (HRMS) in which the electrospray (ESI) technique was used for the ionization. The samples were introduced into the mass spectrometer through a BEH C18 column (50 mm × 2.1 mm × 1.7 μm). A gradient elution of methanol and water (0.3 mL min^{-1}) was used as the mobile phase. All the spectra were recorded in both positive and negative ionization modes in mass-to-charge (*m*/*z*) ranges of 50–600 Da.

2.4. Pulse radiolysis experiments

Time resolved transient spectroscopic studies of the intermediates were carried out on a 7 MeV linear electron accelerator (AS & E, USA) connected to an optical absorption detection system (Luzchem, Canada) which consists of a Cermax parallel lamp (175 W), a monochromator and Hamamastu photomultiplier (R-7400U-04). The dose per pulse of the electron beam

was determined by KSCN dosimetry as per the reported procedure and was found to be around 16 Gy per 100 ns pulse.[37] The transient species generated as a result of pulse irradiation was monitored by time resolved UV-Visible spectroscopy. All other details of the accelerator and detection system have been published elsewhere.[38] Formation processes of primary radicals along with ionic and molecular species by radiolysis of water and the creation of an oxidative environment by removing reducing species using N_2O gas are given in eqn (1) and (2).[23]

$$H_2O \rightsquigarrow {}^{\bullet}OH\ (0.28), H^{\bullet}\ (0.06), e_{aq}{}^{-}(0.27), H^{+}\ (0.27), H_2\ (0.05), H_2O_2\ (0.07) \quad (1)$$

$$e_{aq}{}^{-} + N_2O + H_2O \rightarrow N_2 + {}^{\bullet}OH + {}^{-}OH \quad (2)$$

The values given in parentheses are called *G*-values which represent the number of species formed per 100 eV of incident radiation.[18,23]

3. Results and discussion

3.1. Steady state degradation studies

Preliminary experiments were performed to evaluate the efficiency of $^{\bullet}OH$ mediated destruction of this drug. The initial concentration of theophylline for these experiments was fixed as 1×10^{-5} mol dm^{-3} in order to have a workable sensitivity for the HPLC-DAD system, however, this is considerably higher than the reported concentration of pharmaceutical compounds in water.[21,22] The photo-irradiation in the presence of H_2O_2 results in a complete disappearance of theophylline within 8 min. Fig. 1 shows the degradation profile of this compound as a function of irradiation time. At this timescale, the destruction of theophylline by the direct effect of UV radiation is not significant (data not shown).

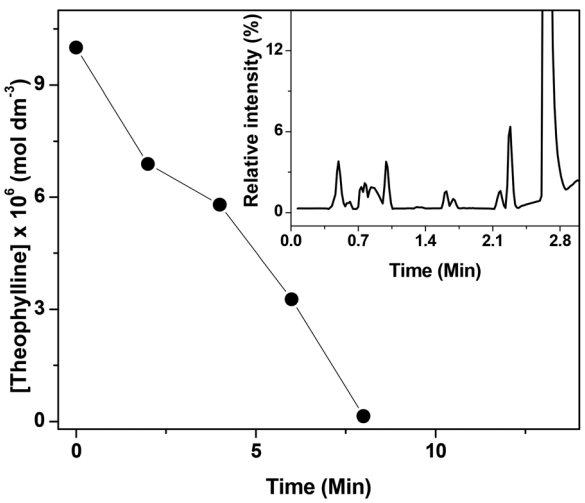

Fig. 1 Photo-degradation profile of theophylline in the presence of H_2O_2 as a function of time. $[theophylline]_0 = 1 \times 10^{-5}$ mol dm^{-3}; $[H_2O_2]_0 = 5 \times 10^{-5}$ mol dm^{-3}. (Inset) Total ion chromatogram of theophylline after H_2O_2/UV photolysis. ($[theophylline]_0 = 1 \times 10^{-4}$ mol dm^{-3}; transformation of theophylline = 37.5%).

It is well-known that photolysis of H_2O_2 yields $^{\bullet}OH$ (eqn (3)).[23] The entire degradation is thus attributed to the oxidation reaction initiated by $^{\bullet}OH$.

$$H_2O_2 + h\nu \rightarrow 2{}^{\bullet}OH \quad (3)$$

The efficient destruction of this compound induced by $^{\bullet}OH$ is very promising especially for the remediation of this pollutant from the aquatic environment. On the other hand, this kind of degradation may not lead to a complete mineralisation of the pollutants. It may also result in a number of intermediate products which may be hazardous too. Considering these possibilities, it is proposed that a thorough understanding of the kinetic and mechanistic aspects of the reaction leading to the destruction of this compound is very important and should be evaluated.

3.2. Product analysis

One convenient method of end product profiling is the use of a high resolution mass spectrometric (HRMS) method such as LC-Q-TOF-MS which provides the accurate masses of each compound. Another advantage of LC-Q-TOF-MS is the ability to analyze highly complex samples without any pre-purification. LC-Q-TOF-MS analyses were carried out on a number of photo irradiated samples in which nearly 20–60% of the parent compound was transformed into different products. To enhance the possibility of detecting minor products that are expected to be in very low concentrations, an initial concentration of 1×10^{-4} mol dm^{-3} theophylline is employed for product studies. The Total Ion Chromatogram (TIC) of theophylline after 6 min of UV irradiation in the presence of H_2O_2 is shown in Fig. 1.

The peak with *m*/*z* 181 (obs. mass 181.0727; calcd for $C_7H_9N_4O_2$ is 181.0726) in positive mode (ESI+) and 179 (obs. mass 179.0565; calcd for $C_7H_7N_4O_2$ is 179.0569) in negative mode (ESI−) represents the parent molecule (data not shown). All other peaks in the TIC stand for various oxidation products of theophylline. To gain further structural features of various peaks in the TIC, MS/MS studies were carried out. The primary products formed during the reaction of theophylline with $^{\bullet}OH$ comprise a hydroxylation product (**i**) and two isomeric demethylation products (**ii** & **iii**). Compound **i** (1,3-dimethyluric acid), the major product of this reaction, was characterized by an intense peak at *m*/*z* 197 (obs. mass 197.0675; calcd for $C_7H_9N_4O_3$ 197.0675) in ESI+ and 195 (obs. mass 195.0510; calcd for $C_7H_7N_4O_3$ 195.0518) in ESI−. The demethylation products, 1-methylxanthine (**ii**) and 3-methylxanthine (**iii**), show peaks at *m*/*z* 167 (obs. mass 167.0567; calcd for $C_6H_7N_4O_2$ 167.0569) in ESI+ and 165 (obs. mass 165.0412; calcd for $C_6H_5N_4O_2$ 165.0413) in ESI−. The substantial difference in the MS/MS spectra (Fig. S1 and S2, ESI†) permits the identification of **iii** and **iv** using tandem mass spectrometry. Further transformation of the primary products results in isomeric uric acids like 1-methyluric acid (**iv**), 3-methyluric acid (**v**) or xanthine (**vi**). The uric acids (**iv** and **v**) show peaks at *m*/*z* 183 (obs. mass 183.0518; calcd for $C_6H_7N_4O_3$ 183.0518) in ESI+

and 181 (obs. mass 181.0360; calcd for $C_6H_5N_4O_3$ 181.0362) in ESI− while the mass spectra of xanthine (**vi**) exhibits an intense peak at *m*/*z* 153 (obs. mass 153.0410; calcd for $C_5H_5N_4O_2$ 153.0413) in ESI+ and 151 (obs. mass 151.0254; calcd for $C_5H_3N_4O_2$ 151.0256) in ESI−. Compounds **i–vi** are previously accounted as microbial metabolites of theophylline.[39] The probable mechanism leading to the formation of these compounds are briefly discussed in section 3.4. In addition to these products (**i–vi**), eight more transformation products (**vii–xiv**) have been identified. Most of these compounds likely originated from the opening of the imidazole ring of theophylline by $^{\bullet}$OH. The entire list of transformation products, with molecular weight and elemental composition, identified by LC-Q-TOF-MS analysis is given in Table 1. The proposed chemical structures of the identified products are presented in Scheme 2. The mass spectra and MS/MS patterns of the transformation products of theophylline are given in the ESI (Fig. S1–S16†).

3.3. Pulse radiolysis studies

In order to obtain more insight into the kinetic and mechanistic aspects of a reaction, the information concerning the short lived intermediates (*i.e.*, initial stages of reaction) is of utmost importance. Pulse radiolysis is the ultimate technique for monitoring the short lived transient species in a nano/micro second time scale.[15] The combination of pulse radiolysis and mass spectrometric techniques is proven as the ideal methodology for obtaining valuable mechanistic insights.[5,6,17] The pK_a value of theophylline was initially determined by plotting the dependence of absorbance at 272 nm (λ_{max} of theophylline) against the pH of the solution (Fig. 2). Theophylline thus exhibits two distinct pK_a (Fig. 2); at 3.3 and 9.8 corresponding to the protonation and deproptonation of NH group respectively.

Table 1 List of transformation products identified by LC-Q-TOF-MS analysis

Sl. no.	Product	Mol. wt.	Elemental composition
i	1,3-Dimethyluric acid	196.16	$C_7H_8N_4O_3$
ii	1-Methylxanthine	166.14	$C_6H_6N_4O_2$
iii	3-Methylxanthine	166.14	$C_6H_6N_4O_2$
iv	1-Methyluric acid	182.14	$C_6H_6N_4O_3$
v	3-Methyluric acid	182.14	$C_6H_6N_4O_3$
vi	Xanthine	152.11	$C_5H_4N_4O_2$
vii	1/3-Methyltetrahydro-1*H*-purine-2,6-dione	168.15	$C_6H_8N_4O_2$
viii	8-Hydroxy-1/3-methyl-3,7,8,9-tetrahydro-1*H*-purine-2,6-dione	184.15	$C_6H_8N_4O_3$
ix	5/6-Amino derivative of 5/6-hydroxy-1,3-dimethylpyrimidine-2,4(1*H*,3*H*)-dione	171.15	$C_6H_9N_3O_3$
x	5/6-Amino derivative of 1/3-methylpyrimidine-2,4(1*H*,3*H*)-dione	141.13	$C_5H_7N_3O_2$
xi	5/6-Aminopyrimidine-2,4(1*H*,3*H*)-dione	127.10	$C_4H_5N_3O_2$
xii	5/6-Amino derivative of 5/6-hydroxy-dihydropyrimidine-2,4(1*H*,3*H*)-dione	145.12	$C_4H_7N_3O_3$
xiii	1/3-Methylpyrimidine-2,4(1*H*,3*H*)-dione	126.11	$C_5H_6N_2O_2$
xiv	5,6-Diaminopyrimidine-2,4(1*H*,3*H*)-dione	142.12	$C_4H_6N_4O_2$

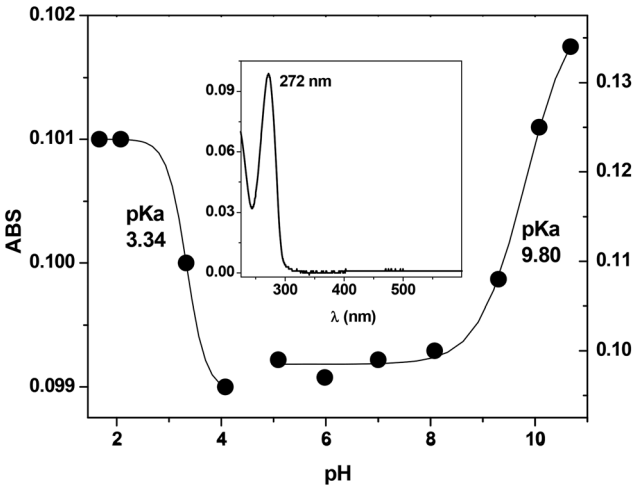

Fig. 2 Plot of pH *vs.* absorbance at 272 nm. (Inset) UV-Vis spectrum of theophylline.

3.3.1. Reaction with hydroxyl radicals. Pulse radiolysis of N_2O saturated solution of theophylline at pH 5.9 yielded a transient absorption spectrum having a sharp absorption maximum at 330 nm and a broad absorption around 500 nm (Fig. 3). The absorption band at 500 nm completely decays within 100 μs with a first order rate constant of 4.91×10^4 s^{-1}. Conversely the absorption band at 330 nm shows a slow decay (Fig. 3). The bimolecular rate constant corresponding to the reaction of theophylline with hydroxyl radical was determined by following the growth of the transient at the 330 nm within a concentration range of (0.5–1) × 10^{-4} mol dm^{-3}. A rate constant of (8.22 ± 0.03) × 10^9 dm^3 mol^{-1} s^{-1} is obtained for this reaction (Fig. 4).

Alternatively, the transient absorption spectrum at pH 10.2 (above pK_a) shows a red shift (λ_{max}: 340 nm; k_2: (7.11 ± 0.07) ×

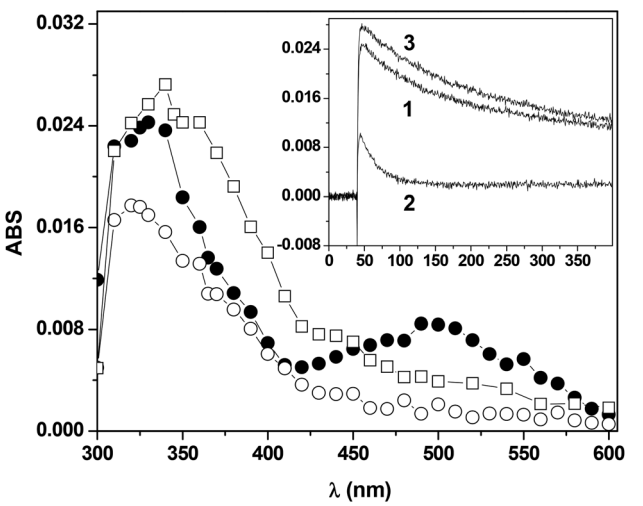

Fig. 3 Transient absorption spectrum recorded during the reaction of $^{\bullet}$OH with theophylline (1 × 10^{-4} mol dm^{-3}) at pH 5.9 after (●) 10 and (○) 100 μs and at pH 10.2 (□) after 10 μs of the pulse. (Inset) Decay traces at (1) 330 nm (pH 5.9), (2) 500 nm (pH 5.9) and (3) 340 nm (pH 10.2).

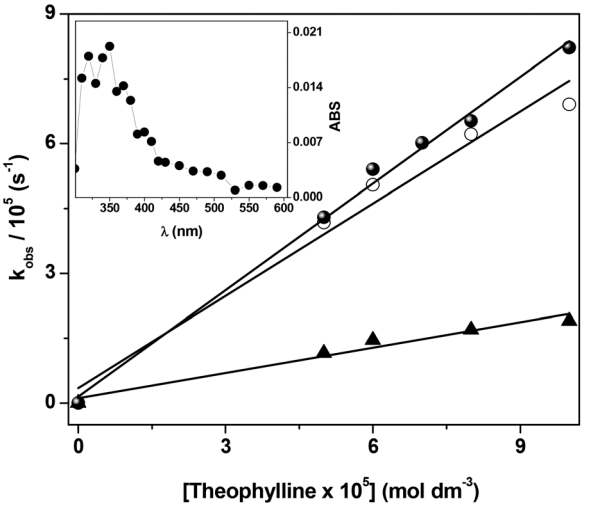

Fig. 4 Plot of k_{obs} against [theophylline] in the case of the reaction of $^{\bullet}OH$ at pH (●) 5.9 (330 nm), (○) 10.2 (340 nm) and (▲) $O^{\bullet-}$ (350 nm). (Inset) Transient absorption spectrum recorded during the reaction of $O^{\bullet-}$ with theophylline (1×10^{-4} mol dm^{-3}) after 20 μs of the pulse.

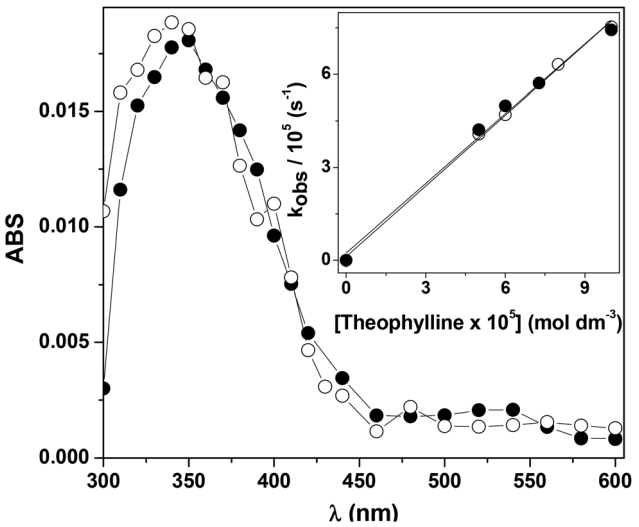

Fig. 5 Transient absorption spectrum of theophylline (1×10^{-4} mol dm^{-3}) recorded during its reaction with $SO_4^{\bullet-}$ after (●) 7 μs (pH 6.0) and with $N_3^{\bullet}$ after (○) 6 μs (pH 6.1). (Inset) Plot of k_{obs} against [theophylline] in the case of reaction of (●) $SO_4^{\bullet-}$ (350 nm) and (○) $N_3^{\bullet-}$ (340 nm).

10^9 dm^3 mol^{-1} s^{-1}) in the UV region lacking any significant absorption in the visible region (Fig. 3).

3.3.2. Reaction with oxide radical. The oxide radical anion ($O^{\bullet-}$) predominantly undergoes one electron transfer and/or hydrogen abstraction reactions.[23] A comparison of the intermediate spectra from this reaction would help in the identification of the intermediate species from $^{\bullet}OH$ reaction. The transient absorption spectrum obtained from the reaction of $O^{\bullet-}$ (at pH > 13) is characterized by two absorption bands at 320 nm and 350 nm (Fig. 4) without having any noteworthy change in the decay profile (Fig. S17, ESI†). At pH > 13, more than 90% of the hydroxyl radicals are converted into $O^{\bullet-}$ with a pK_a value of 11.9 according to the following equation.

$$^{\bullet}OH + {}^{-}OH \leftrightarrow O^{\bullet-} + H_2O \quad (4)$$

The calculated bimolecular rate constant for the reaction of $O^{\bullet-}$ with theophylline from the formation kinetics (Fig. 4) at 350 nm is $(1.95 \pm 0.02) \times 10^9$ dm^3 mol^{-1} s^{-1}.

3.3.3. Reaction with specific one electron oxidants. Being very selective in their reactions, sulfate radical anion ($SO_4^{\bullet-}$) and azide radical ($N_3^{\bullet}$) are ideal for evaluating the contribution of electron transfer reactions in the case of $^{\bullet}OH$ reaction. Generation of $SO_4^{\bullet-}$ and $N_3^{\bullet}$ by pulse radiolysis is exemplified in reactions 5–7.[40–42]

$$(CH_3)_3COH + {}^{\bullet}OH \rightarrow {}^{\bullet}CH_2(CH_3)_2COH + H_2O \quad (5)$$

$$S_2O_8^{2-} + e_{aq}^{-} \rightarrow SO_4^{\bullet-} + SO_4^{2-} \quad (6)$$

$$N_3^{-} + {}^{\bullet}OH \rightarrow N_3^{\bullet} + {}^{-}OH \quad (7)$$

Reaction of $SO_4^{\bullet-}$ at pH 6.0 yielded a transient absorption spectrum having a broad absorption band around 320–380 nm region (Fig. 5). A bimolecular rate constant of $(7.51 \pm 0.04) \times 10^9$ dm^3 mol^{-1} s^{-1} is obtained for this reaction (Fig. 5).

The reaction of sulfate radical with theophylline at a more basic pH (9.3) also shows an absorption band at the same region (data not shown) though the bimolecular rate constant ($k_2 = (5.37 \pm 0.03) \times 10^9$ dm^3 mol^{-1} s^{-1}) obtained in this case is somewhat lower.

Transient absorption spectra having complementary nature were obtained in the case of the reaction of $N_3^{\bullet}$ at pH 6.1 (Fig. 5), 4.0 and 9.5 (data not shown). The bimolecular rate constant obtained at pH 6.1 ($k_2 = (7.61 \pm 0.02) \times 10^9$ dm^3 mol^{-1} s^{-1}) and 9.6 ($k_2 = (8.42 \pm 0.06) \times 10^9$ dm^3 mol^{-1} s^{-1}) are very similar. However, the rate constant value obtained at pH 4 ($k_2 = (4.05 \pm 0.02) \times 10^9$ dm^3 mol^{-1} s^{-1}) is reduced to nearly half. It is noteworthy to mention the fast decay of the transient, with a first order rate constant (k_{obs}) of 3.0×10^4 s^{-1}, at pH 6 though a moderately slow decay is observed in the case of reaction of $SO_4^{\bullet-}$. The substantial variation in the decay profile of the transient in the case of $SO_4^{\bullet-}$ is accounted by interference caused by the absorption of $SO_4^{\bullet-}$ from the UV region. It is also worth mentioning the similarities of both spectra ($SO_4^{\bullet-}$ and $N_3^{\bullet}$) at longer timescales (less interference of $SO_4^{\bullet-}$; Fig. S18, ESI†). The spectral and kinetic parameters of different radicals on its reaction with theophylline are summarized in Table S1 of the ESI.†

As a consequence of the structural similarities of theophylline with purine, it is presumed to go through a similar reaction protocol with $^{\bullet}OH$. Recent works of Chatgilialoglu and coworkers recommended that the main site of hydroxyl radical attack at the base part of the guanosine and deoxyguanosine moiety is the exocyclic amino group (~65%) whereas the hydroxylation at the C8 (~17%) position plays only a minor role.[9,10] The lack of an amino group in theophylline results in the primary reaction of the hydroxyl radical at carbon 8 to form the corresponding hydroxyl radical adduct of the form $(T8\text{-}OH)^{\bullet}$ represented in Scheme 1. The analogous stable

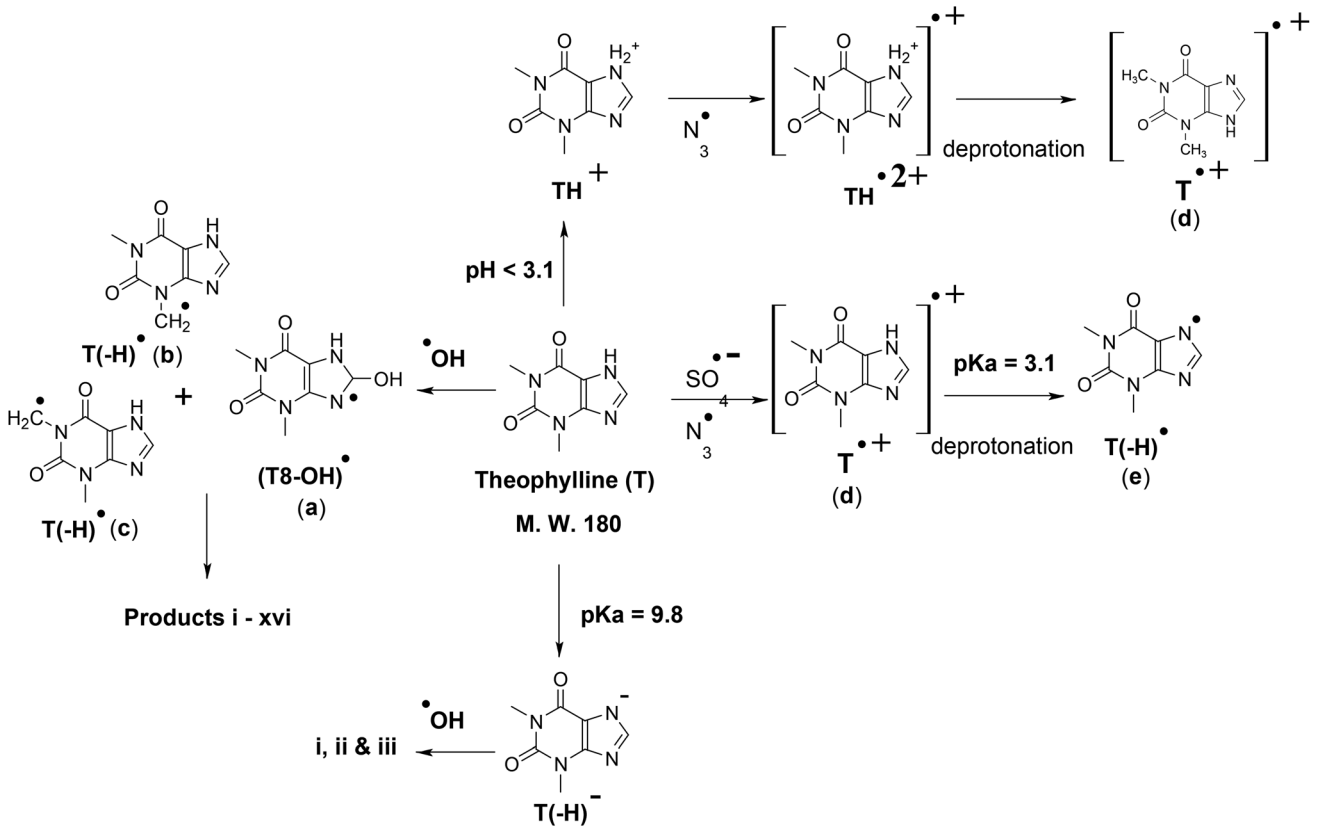

Scheme 1 Proposed mechanism of the reaction of $^{\bullet}OH$, $SO_4^{\bullet-}$, $N_3^{\bullet}$ and $O^{\bullet-}$ with theophylline.

product, 1,3-dimethyluric acid (**i**), identified in our end product studies further supports this assignment. The generation of a similar kind of radical is formerly reported in the case of the oxidation of caffeine.[43]

The C8-OH adduct of (deoxy) guanosine generally undergoes (i) opening of the imidazole ring (yields compounds like 2,6-diamino-4-hydroxy-5-formamidopyrimidine, commonly referred as FapyG)[10] and (ii) bimolecular transformation to 8-oxoguanine.[10] Product studies using LC-Q-TOF-MS show analogous compounds corresponding to these reactions suggesting the feasibility of both processes in the present case. When the samples after pulse irradiation were subjected to end product studies, demethylated products like 1- and 3-methylxanthine (**ii** and **iii**), were detected. Demethylation is supposed to begin with hydrogen abstraction (see section 3.4.2), the contribution of radical(s) generated by hydrogen abstraction from the methyl side chains of theophylline is expected in the transient spectrum. Therefore, it is proposed that the experimental spectrum observed in the case of reaction of $^{\bullet}OH$ with theophylline has a contribution from the radicals **b** and **c** in addition to the primary radical **a**. The evidence for the absorbance of the radicals **b** and **c** came from the interpretation of the transient spectrum resulting from the reaction of $O^{\bullet-}$, which is known to generate hydrogen abstracted species selectively[23] (discussion follows). The exact contribution of these individual radicals is difficult to predict. However, it is assumed that the main absorbing species is the radical **a** since it is well known that $^{\bullet}OH$ predominantly undergoes addition with similar compounds and such adduct radicals exhibit characteristic absorption bands in this region.[10,12,15,18] On the other hand, the slow decay observed at 330 nm compared to 500 nm at pH 6 (Fig. 3) could be due to the interference of the radicals **b** and **c**. It is also predicted that the weak absorption around 500 nm is the contribution of radical **a** since there is no information on the formation of other OH adduct radicals as demonstrated in our LC-Q-TOF-MS results.

At higher alkaline pH, theophylline exists as its deprotonated form represented as $(T-H)^-$ ($pK_a \sim 9.8$) in Scheme 1. The transient absorption spectrum recorded in the case of reaction of $^{\bullet}OH$ with theophylline at pH 10.2 was different from that of pH 6.0 by a red shift in the λ_{max} and a higher absorbance value at UV region (Fig. 3). A similar shift in λ_{max} and absorbance values was also noticed in the ground state absorption spectrum of theophylline (Fig. S19, ESI†). The product profile obtained from the high resolution mass spectrometer is nearly the same as that at pH 6.0 apart from the lack of ring-opened products like **ix**. Since 1,3-dimethyluric acid is also detected at this pH, the addition of $^{\bullet}OH$ at carbon 8 is likely responsible for the transient absorption. The plot of absorbance corresponding to this transient (monitored at 330 nm) as a function of pH gave a clear pK_a curve having an inflection point around pH 10.0 (Fig. S20, ESI†). Differences in the transient spectrum of theophylline on its reaction with $^{\bullet}OH$ at pH 10.2 is thus explained on the basis of the deprotona-

tion of the (T8-OH)$^{\bullet}$. A similar mechanism is previously reported in the case of a series of pyrimidine derivatives.[12] The lack of product **ix** at pH 10.2 indicates the less feasibility of the ring opening reaction of (T8-OH)$^{\bullet}$ above the pK_a of theophylline.

It is well-known that one electron oxidants such as $N_3^{\bullet}$ and $SO_4^{\bullet-}$ results radical cations on its reaction with purines and other aromatic systems.[15,44] Because of the high Brønsted acidity, the radical cation thus formed either reacts with H_2O/OH^- (depends on pH) and yields a hydroxyl radical adduct or is deprotonated into a neutral radical.[15,45] If the former is the case, the corresponding transient spectra should match with the one obtained with $^{\bullet}OH$ reaction. However, it is not observed in the present case (Fig. 3 and 5). In addition, the end product studies on the photo-irradiated samples in the presence of $K_2S_2O_8$ (generates $SO_4^{\bullet-}$ in the medium)[45] did not provide any evidence for the formation of 1,3-dimethyluric acid (see section 3.4.2). The remaining possibility is the deprotonation of the radical cation in to a neutral radical represented as T(−H)$^{\bullet}$ (**e**). Previous studies by Santos *et al.* in the case of one-electron oxidized methylxanthines recommended the formation of a N_7 deprotonated neutral radical with significant stability.[46]

The studies on the fate of radical cations are pertinent in biological systems because of their involvement in diseases like cancer.[47,48] To gain more insight into mechanistic aspects of the deprotonation of the radical cation, the absorbance of the transient at 340 nm obtained in the case of reaction of theophylline with $N_3^{\bullet}$ were monitored as a function of pH. The result is shown in Fig. 6. The inflection point at pH 3.1 obtained by this experiment suggests the existence of a radical cation, without deprotonation, only below pH 3.1. The determined pK_a value of theophylline radical cation is very close to that of guanine.[15,44]

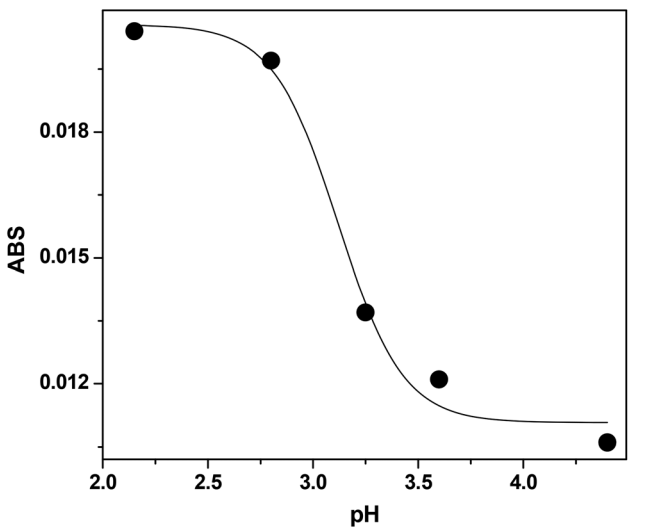

Fig. 6 Plot of absorbance of the transient at 340 nm against pH in the case of reaction of $N_3^{\bullet-}$.

Another explanation for the existence of radical cations at highly acidic pH is that the protonated form of theophylline (pK_a ~ 3.3), represented as TH^+, undergoes one electron oxidation with $N_3^{\bullet}$ to form a $TH^{\bullet 2+}$ (**f**). The $TH^{\bullet 2+}$ is expected to be highly unstable and instantly releases a proton to yield theophylline radical cation ($T^{\bullet+}$). Hence, the broad absorption band obtained between 320–380 nm in the case of the reaction of $N_3^{\bullet}$ and $SO_4^{\bullet-}$ (Fig. 5) at neutral and basic pH is assigned to the N_7 deprotonated neutral radical T(−H)$^{\bullet}$ (Scheme 1).

One electron transfer and/or hydrogen abstraction reactions are reported as the primary route of the reaction of $O^{\bullet-}$ with aromatic compounds.[23] If electron abstraction occurs, an N_7 deprotonated radical (**e**) will be a possible intermediate. Since the reaction of theophylline with specific one electron oxidants, that is $SO_4^{\bullet-}$ and $N_3^{\bullet}$, also generates the same radical, a similar spectrum is presumed. However, this is not observed in the present case (Fig. 4 and 5). The only remaining possibility is the abstraction of a hydrogen atom from either of the methyl side chains of theophylline to form another carbon centered T(−H)$^{\bullet}$ radical (**b** or **c**). Hence, the absorption bands obtained in the present case are likely due to the formation of radicals **b** or/and **c**. It is also worth mentioning the low bimolecular rate constant (k_2 = (1.95 ± 0.02) × 10^9 dm^3 mol^{-1} s^{-1}) determined for this reaction (k_2 values corresponding to the hydrogen abstraction reactions are usually low).[23]

3.4. Reaction mechanism

The various transformation products corresponding to the reaction of $^{\bullet}OH$ with theophylline have already been discussed in section 3.2. The transformation pathways of theophylline on its reaction with $^{\bullet}OH$ are classified into three stages (stage 1–3) and are described in Scheme 2. Stage 1 explains the formation of the primary products of theophylline (Schemes 3 and 4) whereas stage 2 and 3 explain further transformation of the primary products. The mechanism of formation of the primary products induced by $^{\bullet}OH$ are separately discussed in Schemes 3 and 4.

3.4.1. Hydroxylation. The primary transformation product of the reaction of $^{\bullet}OH$ with theophylline, irrespective of reaction conditions, is 1,3-dimethyluric acid (**i**). That is the one corresponding to hydroxylation of the parent molecule at carbon 8. The nearly diffusion controlled bimolecular rate constant (k_2 = (8.22 ± 0.03) × 10^9 dm^3 mol^{-1} s^{-1}) corresponding to the reaction of theophylline with $^{\bullet}OH$ determined during the pulse radiolysis studies is in accordance with the hydroxylation possibility (section 3.3.1). Previous studies on structurally similar molecules, such as caffeine and guanine, also pointed to a similar protocol.[9,15,43]

The mechanism of the formation of this compound involves one electron oxidation of the early intermediate (T8-OH)$^{\bullet}$ followed by deprotonation (Scheme 3). The OH radical adduct of guanine also undergoes an analogous mechanism that leads to the formation of 8-oxo-G,[49] a widely used biomarker for oxidative stress.[9,15]

3.4.2. Demethylation. Products corresponding to demethylation of the methyl side chains of theophylline, that is 1 and 3-methylxanthine (**ii** and **iii**, both having M.W. 166.14 but

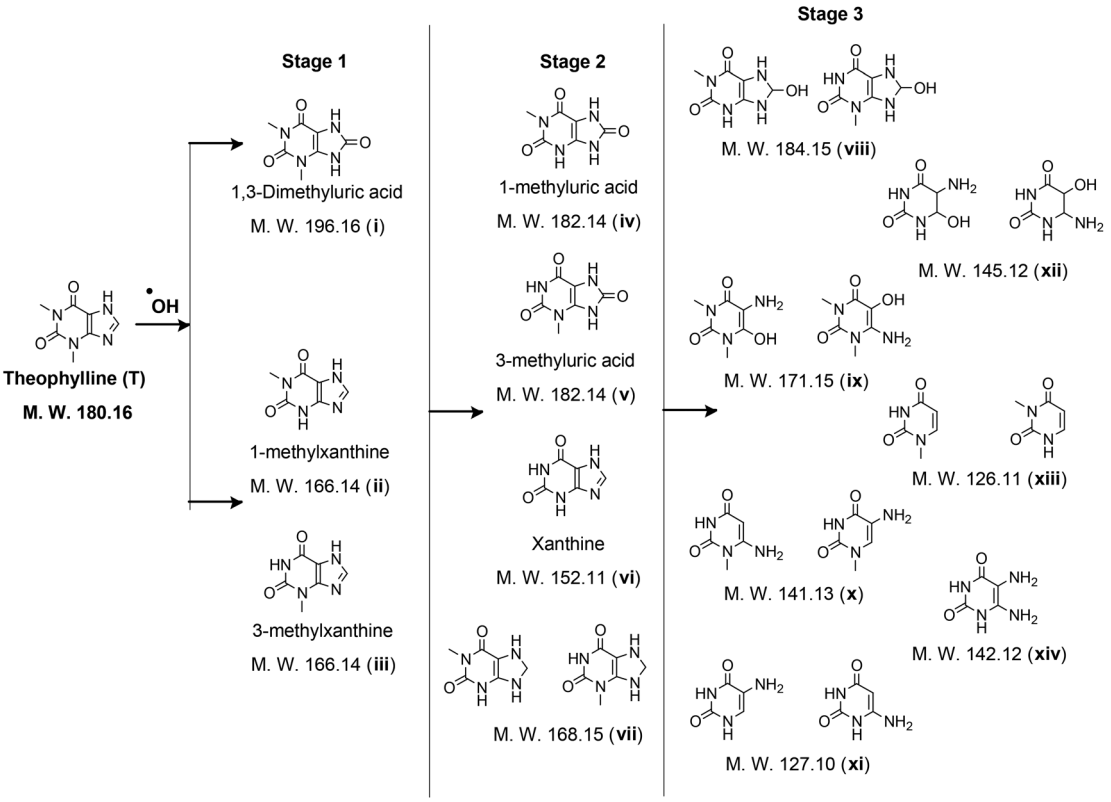

Scheme 2 Proposed degradation pathways of theophylline on its reaction with •OH.

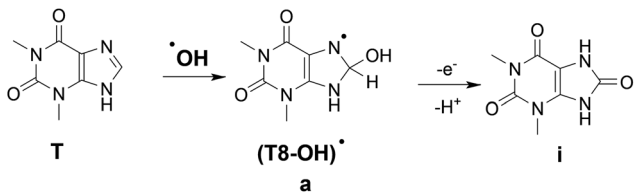

Scheme 3 Mechanism of the formation of 1,3-dimethyluric acid from theophylline.

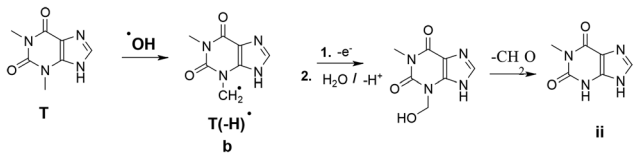

Scheme 4 Mechanism of the formation of 1-methylxanthine from theophylline.

different fragmentation pattern, Fig. S1 and S2, ESI†), are important minor products in this reaction. This transformation is of biological relevance because of the potent antioxidant activities of methylxanthines.[36] Two distinct mechanisms *viz.* hydrogen abstraction and one electron oxidation are proposed as the gateway to demethylation.[36,50] To account for the contribution of one electron oxidation in this process, end product studies were carried out in photo-irradiated samples of theophylline (1×10^{-4} mol dm^{-3}) in the presence of 1×10^{-3} mol dm^{-3} $K_2S_2O_8$. Sulfate radical anion ($SO_4^{\bullet -}$), a specific one electron oxidant, is the reacting species in this case.[45] If one electron oxidation is the fundamental mechanism, **ii** and **iii** are expected in the end product profile. However, the targeted MS/MS analysis using LC-Q-TOF-MS did not give any information towards the formation of **ii** and **iii**. The involvement of one electron oxidation is thus eliminated from this case. The remaining possibility is hydrogen abstraction. A multi-step mechanism is proposed by Santos and co-workers for this conversion.[36] The first step of the mechanism involves the hydrogen abstraction from one of the methyl side chains (for example: N_3–CH_3 in Scheme 4) to form a carbon centered radical (**b**). An instant electron release from radical **b** followed by hydrolysis generates a hydroxymethyl intermediate compound. The liberation of hydroxymethyl groups from this intermediate results in the corresponding demethylated compound (**ii**).

3.4.3. Other products. The products **iv**–**xiv**, generated by the further conversion of the initial products by reactive species, were detected as minor peaks in the TIC. The mechanism of the isomeric uric acids (**iv** and **v**) is explained by two distinct mechanisms. The first one is a hydroxylation–demethylation protocol in which the demethylation of **i**, formed as a result of the hydroxylation of theophylline at carbon 8 (see Scheme 2), at N_1 and N_3–CH_3 groups respectively results **iv** and **v**. Alternately, a demethylation–hydroxylation protocol is also possible in which hydroxylation of **ii** and **iii** at carbon 8 results in the corresponding products. Likewise, demethylation of **ii** and **iii** results in xanthine (**vi**) (Scheme 5).

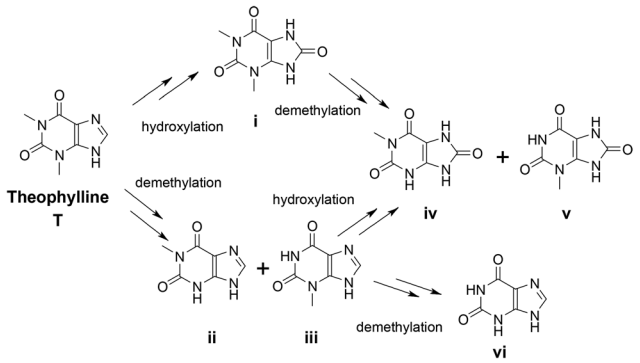

Scheme 5 Formation of xanthine and methyluric acids from theophylline.

As the photo-irradiation proceeds, the concentrations of some of the transformation products such as **i** could be equal (or even exceed) that of the parent compound. Hence the probability of $^{\bullet}OH$ attack on the initially formed products rises. Similar observations were previously reported in the case of many organic compounds.[5,6,17]

The opening of the imidazole ring of $(T8\text{-}OH)^{\bullet}$ is presumed to be responsible for the formation of compounds **ix–xiv**. Analogous reactions are well studied in the case of the hydroxyl radical adduct of guanine derivatives which leads to the formation of products such as FapyG.[9,10,15] However, compounds like **vii** and **viii**, detected at extremely trace level, are not usually found in oxidative conditions. The mechanism corresponding to the formation of such products, observed in reducing conditions, in the present case is not clear. The possible side-reactions associated with H_2O_2 or the direct photo reduction of some of the initially formed products of theophylline (such as **ii–v**) by UV radiation is a likely reason for this conversion. The photo-transformation of aldehydes and ketones to the corresponding alcohols are familiar in synthetic chemistry.[51] Moreover, the high sensitivity of LC-Q-TOF-MS allows the detection of such minor products without compromising the mass accuracy.

It is worth noting that nearly 20% reduction in the photo degradation efficiency (at 6 min) is observed in the case of H_2O_2/photolysis in N_2 purged (that is deaerated) medium (Fig. S21, ESI†). The high reactivity of $(A8\text{-}OH)^{\bullet}$ of N_6,N_6-dimethyladenosine towards molecular oxygen is well known.[52] A likely reason for the enhanced degradation efficiency in an aerated medium is the involvement of molecular oxygen in the reaction mechanism. This result is especially important because of the presence of molecular oxygen in most of the biological and environmental systems in which reactions of $^{\bullet}OH$ occurs. Conversely, the concentration of the major oxidation product, 1,3-dimethyluric acid, formed in the case of N_2 purged conditions was significantly higher. It is thus presumed that the presence of molecular oxygen in the medium induces further oxidation of the initially formed products like 1,3-dimethyluric acid.

4. Conclusions

The kinetic and mechanistic aspects of a representative methylxanthine drug, theophylline, against hydroxyl radical ($^{\bullet}OH$) have been explicated by pulse radiolysis and LC-Q-TOF-MS techniques. Two pathways – addition and hydrogen abstraction – are demonstrated for the reaction of $^{\bullet}OH$. The adduct radical $(T8\text{-}OH)^{\bullet}$ undergoes a ring opening reaction and yields products analogous to FapyG (a potential biomarker for oxidative stress). LC-Q-TOF-MS analysis undoubtedly demonstrates the role of hydrogen abstraction also in the initial step of this reaction. This result is rather unusual as $^{\bullet}OH$ generally undergoes addition reaction with similar compounds. Characterization of various transformation products including isomeric xanthines (**ii** & **iii**) and uric acids (**iv** & **v**) by LC-Q-TOF-MS is an important illustration which is generally difficult to achieve. The rapid destruction of theophylline by H_2O_2/UV photolysis is an excellent hint at the vulnerability of this compound against oxidizing radicals. This is an important finding in the context of oxidation technologies for pollutant degradation. However, the efficiency of oxidizing radicals against the complete destruction of the parent as well as the transformed organic compound in natural waters could possibly be reduced due to scavenging of $^{\bullet}OH$ by a variety of inorganic ions and dissolved organic matter. Therefore, additional efforts for assessing the efficiency and toxicity/TOC decline are essential for the practical implementation of these types of methodologies and are presently in progress.

Acknowledgements

We acknowledge National Centre for Free Radical Research, University of Pune, Pune for the pulse radiolysis facility. This work was performed under collaborative research scheme (Ref no. UGC-DAE-CSR-KC/CRS/09/RC02/1455) of UGC-DAE Consortium for Scientific Research, Kolkata Centre, Kolkata. CTA is thankful to DST (under PURSE and FIST scheme) for partial financial support. GP is thankful to SB College, Changanasserry for research guideship.

Notes and references

1 E. Brillas, I. Sirés and M. A. Oturan, *Chem. Rev.*, 2009, **109**, 6570–6631.
2 P. Calza, C. Medana, E. Raso, V. Giancotti and C. Minero, *Rapid Commun. Mass Spectrom.*, 2011, **25**, 2923–2932.
3 J. De Laat, H. Gallard, S. Ancelin and B. Legube, *Chemosphere*, 1999, **39**, 2693–2706.
4 U. Kalsoom, S. S. Ashraf, M. A. Meetani, M. A. Rauf and H. N. Bhatti, *Chem. Eng. J.*, 2012, **200–202**, 373–379.
5 R. Sreekanth, K. P. Prasanthkumar, M. M. Sunil Paul, U. K. Aravind and C. T. Aravindakumar, *J. Phys. Chem. A*, 2013, **117**, 11261–11270.

6 M. M. Sunil Paul, U. K. Aravind, G. Pramod and C. T. Aravindakumar, *Chemosphere*, 2013, **91**, 295–301.
7 D. C. McDowell, M. M. Huber, M. Wagner, U. von Gunten and T. A. Ternes, *Environ. Sci. Technol.*, 2005, **39**, 8014–8022.
8 J. Cadet, T. Douki and J. L. Ravanat, *Free Radicals Biol. Med.*, 2010, **49**, 9–21.
9 C. Chatgilialoglu, M. D'Angelantonio, G. Kciuk and K. Bobrowski, *Chem. Res. Toxicol.*, 2011, **24**, 2200–2206.
10 C. Chatgilialoglu, M. D'Angelantonio, M. Guerra, P. Kaloudis and Q. G. Mulazzani, *Angew. Chem., Int. Ed.*, 2009, **48**, 2214–2217.
11 A. Kumar, V. Pottiboyina and M. D. Sevilla, *J. Phys. Chem. B*, 2011, **115**, 15129–15137.
12 T. L. Luke, T. A. Jacob, H. Mohan, H. Destaillats, V. M. Manoj, P. Manoj, J. P. Mittal, M. R. Hoffmann and C. T. Aravindakumar, *J. Phys. Chem. A*, 2002, **106**, 2497–2504.
13 V. M. Manoj and C. T. Aravindakumar, *Chem. Commun.*, 2000, 2361–2362.
14 P. O'Neill, *Radiat. Res.*, 1983, **96**, 198–210.
15 S. Steenken, *Chem. Rev.*, 1989, **89**, 503–520.
16 J. A. Theruvathu, C. T. Aravindakumar, R. Flyunt, J. von Sonntag and C. von Sonntag, *J. Am. Chem. Soc.*, 2001, **123**, 9007–9014.
17 S. P. Mezyk, T. J. Neubauer, W. J. Cooper and J. R. Peller, *J. Phys. Chem. A*, 2007, **111**, 9019–9024.
18 W. Song, W. J. Cooper, S. P. Mezyk, J. Greaves and B. M. Peake, *Environ. Sci. Technol.*, 2008, **42**, 1256–1261.
19 K. Kummerer, *Chemosphere*, 2009, **75**, 417–434.
20 T. Heberer, *Toxicol. Lett.*, 2002, **131**, 5–17.
21 A. J. Ramirez, R. A. Brain, S. Usenko, M. A. Mottaleb, J. G. O'Donnell, L. L. Stahl, J. B. Wathen, B. D. Snyder, J. L. Pitt, P. Perez-Hurtado, L. L. Dobbins, B. W. Brooks and C. K. Chambliss, *Environ. Toxicol. Chem.*, 2009, **28**, 2587–2597.
22 Y. Vystavna, F. Huneau, V. Grynenko, Y. Vergeles, H. Celle-Jeanton, N. Tapie, H. Budzinski and P. Le Coustumer, *Water, Air, Soil Pollut.*, 2012, **223**, 2111–2124.
23 G. V. Buxton, C. L. Greenstock, W. P. Helman and A. B. Ross, *J. Phys. Chem. Ref. Data*, 1988, **17**, 513–886.
24 L. P. Candeias and S. Steenken, *Chem. – Eur. J.*, 2000, **6**, 475–484.
25 A. J. Szentmiklosi, A. Cseppento, R. Gesztelyi, J. Zsuga, A. Kortvely, G. Harmati and P. P. Nanasi, *Curr. Med. Chem.*, 2011, **18**, 3695–3706.
26 I. I. Koleva, T. A. van Beek, A. E. M. F. Soffers, B. Dusemund and I. M. C. M. Rietjens, *Mol. Nutr. Food Res.*, 2012, **56**, 30–52.
27 B. Stavric, *Food Chem. Toxicol.*, 1988, **26**, 541–565.
28 J. R. León-Carmona and A. Galano, *Int. J. Quantum Chem.*, 2012, **112**, 3472–3478.
29 I. Baranowska and J. Kapinos, *Chem. Anal.*, 2000, **45**, 53–58.
30 B. G. Cosio, A. Iglesias, A. Rios, A. Noguera, E. Sala, K. Ito, P. J. Barnes and A. Agusti, *Thorax*, 2009, **64**, 424–429.
31 K. V. Blake, K. L. Massey, L. Hendeles, D. Nickerson and A. Neims, *Ann. Emergency Med.*, 1988, **17**, 1024–1028.
32 I. Kupsáková, A. Rybár, P. Dočolomanský, Z. Drobná, U. Stein, W. Walther, M. Barančík and A. Breier, *Eur. J. Pharm. Sci.*, 2004, **21**, 283–293.
33 H. Yin, X. Meng, H. Su, M. Xu and S. Ai, *Food Chem.*, 2012, **134**, 1225–1230.
34 T. Antoniou, T. Gomes, M. Mamdani and D. Juurlink, *Eur. J. Clin. Pharmacol.*, 2011, **67**, 521–526.
35 R. Liang, A. Hu, W. Li and Y. N. Zhou, *J. Nanopart. Res.*, 2013, **15**, 1–13.
36 P. Santos, S. Silva, G. Justino and A. Vieira, *Redox Rep.*, 2010, **15**, 138–144.
37 G. V. Buxton and C. R. Stuart, *J. Chem. Soc., Faraday Trans.*, 1995, **91**, 279–281.
38 K. M. S. P. Yadav, M. B. Shirdhonkar and B. S. M. Rao, *Curr. Sci.*, 2007, **92**, 599–605.
39 C. L. Yu, T. M. Louie, R. Summers, Y. Kale, S. Gopishetty and M. Subramanian, *J. Bacteriol.*, 2009, **191**, 4624–4632.
40 P. Manoj, H. Mohan, J. P. Mittal, V. M. Manoj and C. T. Aravindakumar, *Chem. Phys.*, 2007, **331**, 351–358.
41 D. B. Naik and K. Kishore, *Res. Chem. Intermed.*, 2002, **28**, 603–617.
42 T. L. Luke, H. Mohan, V. M. Manoj, P. Manoj, J. P. Mittal and C. T. Aravindakumar, *Res. Chem. Intermed.*, 2003, **29**, 379–391.
43 J. P. Telo and A. J. S. C. Vieira, *J. Chem. Soc., Perkin Trans. 2*, 1997, 1755–1758.
44 K. Kobayashi and S. Tagawa, *J. Am. Chem. Soc.*, 2003, **125**, 10213–10218.
45 P. Neta, R. E. Huie and A. B. Ross, *J.Phys. Chem. Ref. Data*, 1988, **17**, 1027–1284.
46 P. M. P. Santos, J. P. Telo and A. J. S. C. Vieira, *Redox Rep.*, 2008, **13**, 123–133.
47 E. Cavalieri and E. Rogan, *Environ. Health Perspect.*, 1985, **64**, 69–84.
48 A. F. Lehner, J. Horn and J. W. Flesher, *Biochem. Biophys. Res. Commun.*, 2004, **322**, 1018–1023.
49 L. I. Shukla, A. Adhikary, R. Pazdro, D. Becker and M. D. Sevilla, *Nucleic Acids Res.*, 2004, **32**, 6565–6574.
50 P. M. P. Santos, A. M. M. Antunes, J. Noronha, E. Fernandes and A. J. S. C. Vieira, *Eur. J. Med. Chem.*, 2010, **45**, 2258–2264.
51 N. Kambe, K. Kondo, S. Murai and N. Sonoda, *Angew. Chem., Int. Ed. Engl.*, 1980, **19**, 1008–1009.
52 A. J. S. C. Vieira and S. Steenken, *J. Am. Chem. Soc.*, 1987, **109**, 7441–7448.

